Structural and magnetic anisotropy in amorphous alloy ribbons

1997 J. Phys.: Condens. Matter 9 L375

(http://iopscience.iop.org/0953-8984/9/26/001)

J. Phys.: Condens. Matter **9** (1997) L375–L383. Printed in the UK PII: S0953-8984(97)83012-3

LETTER TO THE EDITOR

Structural and magnetic anisotropy in amorphous alloy ribbons

Q A Pankhurst†, L Fernández Barquín†‖, J D Wicks†¶, R L McGreevy‡ and M R J Gibbs§

† Department of Physics and Astronomy, University College London, London WC1E 6BT, UK
‡ Studsvik Neutron Research Laboratory, Uppsala University, S-611 82 Nyköping, Sweden
§ Department of Physics, University of Sheffield, Sheffield S3 7RH, UK

Received 3 April 1997

Abstract. We report x-ray, EXAFS and neutron diffraction experiments on stress-relieved (SR) and field-annealed (FA) ribbons of $Fe_{78}Si_9B_{13}$ using optimized geometries to measure the structural and magnetic anisotropy to unprecedented accuracy. A peak of magnitude ~5% of the main peak height is found in the $\Delta S(Q)$ pattern from three independent neutron experiments on the FA ribbons, at $Q \sim 3$ Å^{-1}. We establish that this peak is of magnetic origin, arising from moments that to some extent lie perpendicularly to the anneal field direction, and is associated with local structure. We show that this anisotropy is consistent with a recently proposed disturbed exchange model, suggesting that the result represents the first direct observation of the existence of antiferromagnetically coupled moments within an amorphous ferromagnetic alloy.

Some FeNi- and Fe-based amorphous alloys have a large magnetostrictive response to low fields coupled with a low macroscopic magnetic anisotropy, making them suitable for state-of-the-art transducer and sensor applications. Both the anisotropy and the magnetostriction may be controlled via post-production treatment such as thermal annealing in an applied field [1, 2]. In $Fe_{78}Si_9B_{13}$ the magnetostriction λ_e can be increased from 30 ppm in as-cast material to 62 ppm by annealing at 400 °C for one hour in a field of 0.4 T; the treatment also increases the magnetic anisotropy K_u from <5 J m^{-3} to 65 J m^{-3} [2]. The microscopic mechanism by which these desirable changes are effected is not yet understood on other than a phenomenological level. A fundamental understanding of the process of inducing magnetic anisotropy is needed both for the exploitation of amorphous alloys, and as a means of testing and refining atomic models of their structure and magnetism. In recognition of this, there have been several neutron diffraction searches for structural and/or magnetic anisotropy in amorphous alloys over the last decade [3–5]. However, except in extreme cases such as under large applied stress or after extended cold-rolling, these have not found any measurable anisotropy.

In this letter we report a new x-ray, EXAFS and neutron diffraction study of the atomic structure of $Fe_{78}Si_9B_{13}$ amorphous ribbons. By using large-area samples with carefully prescribed macroscopic properties, and using specialized detector geometries on a series of complementary neutron and x-ray instruments, we could measure the anisotropy with unprecedented accuracy. We find direct evidence for in-plane structural and magnetic anisotropy induced by the post-production treatment, the nature of which,

‖ Present address: CITIMAC, Facultad Ciencias, Universidad de Cantabria, Santander 39005, Spain.
¶ Present address: Cavendish Laboratory, Madingley Road, Cambridge CB3 OHE, UK.

0953-8984/97/260375+09$19.50

when interpreted using a recently proposed disturbed exchange model [6], provides insights into the microscopic origin of the macroscopic magnetic anisotropy.

The $Fe_{78}Si_9B_{13}$ samples comprised stacks of four rectangular sections, 150 mm × 75 mm × 25 mm, cut from a roll of commercial material, METGLAS® 2605-S2. These 'ultra-wide' continuously cast ribbons (supplied by Allied Chemical Corporation) are advantageous since an incident neutron or x-ray beam can be directed onto an unbroken area of the ribbon plane. The difficulties of stray fields and edge effects, encountered in earlier studies using multiply wound samples of ribbons 1 or 2 mm wide, were therefore avoided. The samples were post-production treated. Field-annealed (FA) ribbons were prepared by sandwiching them between aluminium plates and heating with a hot-air gun to 400 ± 1 °C in an applied field of 0.4 T aligned within $\pm 2^\circ$ of the short (75 mm) axis. After 40 minutes the hot-air gun was turned off, and the sample allowed to cool to room temperature with the field on. Stress-relieved (SR) ribbons were prepared similarly, but with no field applied. In previous work using as-cast ribbons, the inhomogeneous stresses and strains induced during casting made the results difficult to repeat and to interpret. In contrast, both the SR state and the FA state are stable and well defined [7]. This allows comparison of the atomic structure in two structurally relaxed ground states, differing only by the presence or absence of a magnetic field in the thermal anneal.

Complementary x-ray and neutron diffraction experiments were performed. Synchrotron x-ray diffraction measurements were made on Station 9.1 at the Daresbury Laboratory, UK, to probe for features of a purely structural nature. Extended x-ray absorption fine-structure (EXAFS) spectra were recorded on Station 7.1 at the Daresbury Laboratory. This technique is useful in determining chemical and/or topological variations at short range, up to 5 Å, for metallic glasses [8]. Three neutron instruments were used to probe for features of both structural and magnetic origin: the LAD and SANDALS diffractometers at the ISIS Facility spallation source at the Rutherford Appleton Laboratory, UK, and the SLAD diffractometer at the reactor source in the Studsvik Neutron Research Laboratory, Sweden. By using three different neutron instruments we address the issue of systematic errors: those that can arise due to small differences in ribbon thickness and the placement of the sample in the beam, and any bias that might be introduced through data correction and background subtraction procedures. Differences in the optimal Q-ranges for the instruments also allow us to probe both wide-angle data corresponding to local anisotropy, on an atomic length scale, as well as small-angle data relevant to large-scale structure, such as magnetic domain ordering.

For all the diffraction measurements, the samples were mounted so that the in-plane scattering vectors parallel ($Q_\parallel$) and perpendicular ($Q_\perp$) to their short axis (the anneal field direction in the FA ribbons) could be measured and compared. This required careful sample positioning and detector selection on each instrument. Further experimental details are as follows.

(i) The x-ray patterns were collected as an ensemble of successive transmission runs using Warren–Mavel geometry to minimize the Compton scattering [9]. The samples were mounted perpendicularly to the beam and repositioned between runs to randomize any spurious sample mounting effects. Runs were scanned between 2θ-angles of 2° and 80° in 0.01° steps at 4 s per angle using $\lambda = 0.485\,82$ Å.

(ii) Fe K-edge transmission EXAFS runs were performed on single-ribbon samples, and calibrated against an iron foil. Raw data were analysed using the Daresbury EXCALIB, EXBACK and EXCURV92 software packages.

(iii) Initial neutron experiments used the LAD diffractometer [10]. The ribbon plane was tilted at 45° to the incident beam, and only the detectors at ±90° to the beam were consulted.

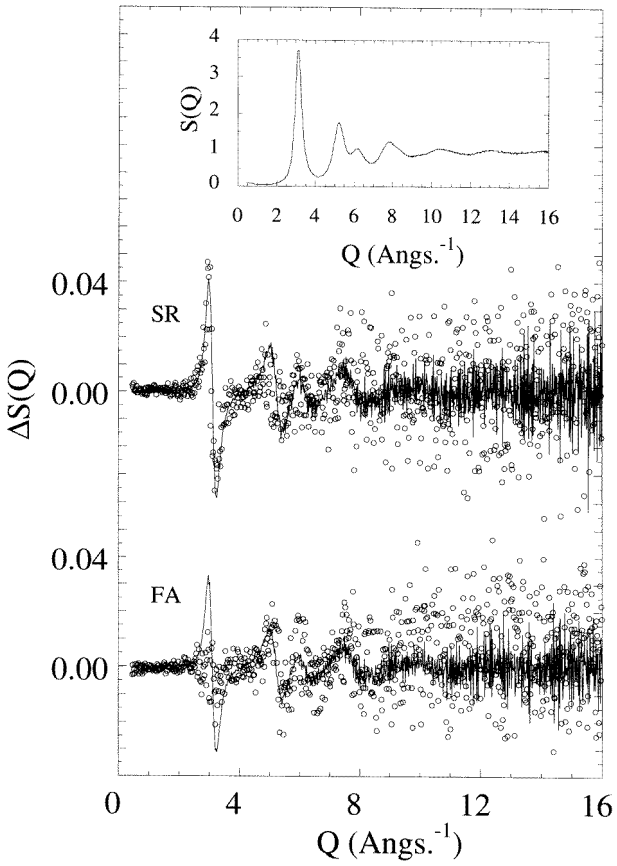

Figure 1. Synchrotron x-ray diffraction data for stress-relieved (SR) and field-annealed (FA) $Fe_{78}Si_9B_{13}$ ribbons: the difference (circles) in structure factors measured with the scattering vector parallel and perpendicular to the anneal field axis, $\Delta S(Q) = S(Q_{\parallel}) - S(Q_{\perp})$, compared with that predicted (solid lines) for structural anisotropy due to uniform internal strain of magnitude 0.11% and 0.09% respectively. Inset: a representative total structure factor $S(Q)$.

This is an advantageous geometry as any two of the three orthogonal scattering vectors lying in and normal to the ribbon plane can be measured simultaneously and independently [11].

(iv) Further data were recorded on SANDALS, which has higher resolution than LAD at low Q. Here the ribbon plane was rotated by $\sim 6^\circ$ about the vertical so that the 9° azimuth detectors at 45° above and below the horizontal plane received data from in-plane scattering vectors which were nearly orthogonal (89.5°). Subsequent data correction, including normalization, absorption and multiple-scattering calculations, was applied using the ATLAS programme suite.

(v) SLAD experiments on the FA sample used the 50 MW reactor source in Studsvik. Unlike the pulsed-source instruments at ISIS, where the detectors were fixed at a constant position and the scattering vectors were kept in the plane for the full $|Q|$-range, on SLAD the scattering vector was exactly in the plane only at a single Q-value, dependent on the sample geometry. Four pairs of runs were completed, with the sample positioned with its normal at $\alpha = 0^\circ, 5^\circ, 15^\circ$ and 30° to the incident beam. The scattering vector was exactly in the plane at $|Q| = 0$ Å^{-1}, 0.99 Å^{-1}, 2.93 Å^{-1} and 5.66 Å^{-1} respectively. Full corrections were

made to the total structure factors, including normalization against a flat-plate vanadium standard.

X-ray diffraction data are shown in figure 1 after normalization, absorption and density corrections. The inset shows a representative total structure factor, $S(Q)$. The difference patterns, $\Delta S(Q) = S(Q_\parallel) - S(Q_\perp)$, of both samples show a series of bimodal oscillation peaks. The largest is of magnitude ∼1% of the main peak height for the SR sample at $Q \sim 3$ Å^{-1}. Smaller features are centred at ∼5 Å^{-1} and 6 Å^{-1} in both samples, coinciding with peaks in $S(Q)$. This behaviour is very similar to experimental and modelling data for FeNi-based ribbons which had been stress annealed to produce a uniform shear strain [12], and a molecular dynamics study of amorphous alloys subject to uniaxial stress [13]. These earlier studies showed that the strain gives rise to a $\Delta S(Q)$ that is proportional to the derivative of the isotropic structure factor, $\Delta S(Q) = Q(\mathrm{d}S_0(Q)/\mathrm{d}Q)\varepsilon$, where ε is the axial shear strain magnitude [12]. To quantify this strain, we have as an approximation used the observed $S(Q)$ as substitute for a truly isotropic $S_0(Q)$, and compared $Q(\mathrm{d}S(Q)/\mathrm{d}Q)$ with $\Delta S(Q)$. This is shown in figure 1 for scaling factors (i.e. strains) of $\varepsilon = 0.11\%$ for the SR ribbons and $\varepsilon = 0.09\%$ for the FA ribbons. The agreement is very good for the SR sample across all Q, and is good for the FA sample for $Q > 4$ Å^{-1}. At smaller Q in the FA sample the observed $\Delta S(Q)$ is consistent with a smaller strain of ∼0.03%, which may imply that in the FA ribbons the strain is not uniform, but smaller over a long range, $\lambda > 3$ Å, with the more local strains being larger, but still reduced compared to the case for the SR sample. This is consistent with the post-production treatment received by both sets of ribbons, which should have removed most of the initial casting stresses.

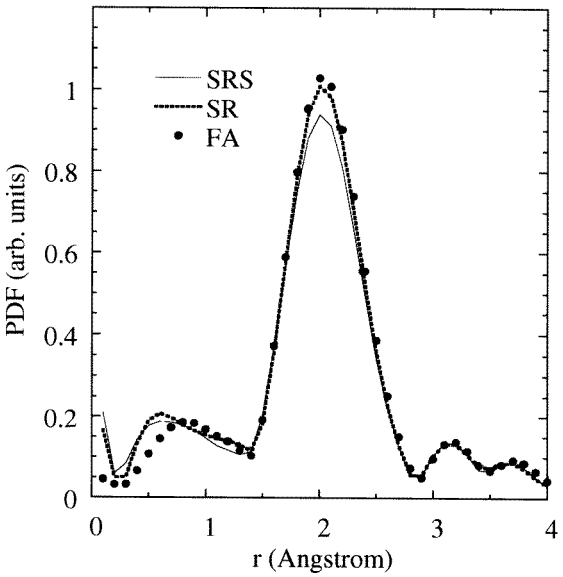

Figure 2. EXAFS pair distribution functions for stress-relieved (SR) and field-annealed (FA) $Fe_{78}Si_9B_{13}$ ribbons, and for a SR ribbon subject to a tensile stress of 5 MPa (SRS).

EXAFS data are shown in figure 2 for the SR and FA ribbons and, for comparison, for a SR ribbon subject to a 5 MPa tensile stress along its long axis. Small differences are evident in the pair distribution functions (PDFs) of the samples, indicating slight but definite changes in atomic arrangement, comparable to the effect of an applied stress of perhaps

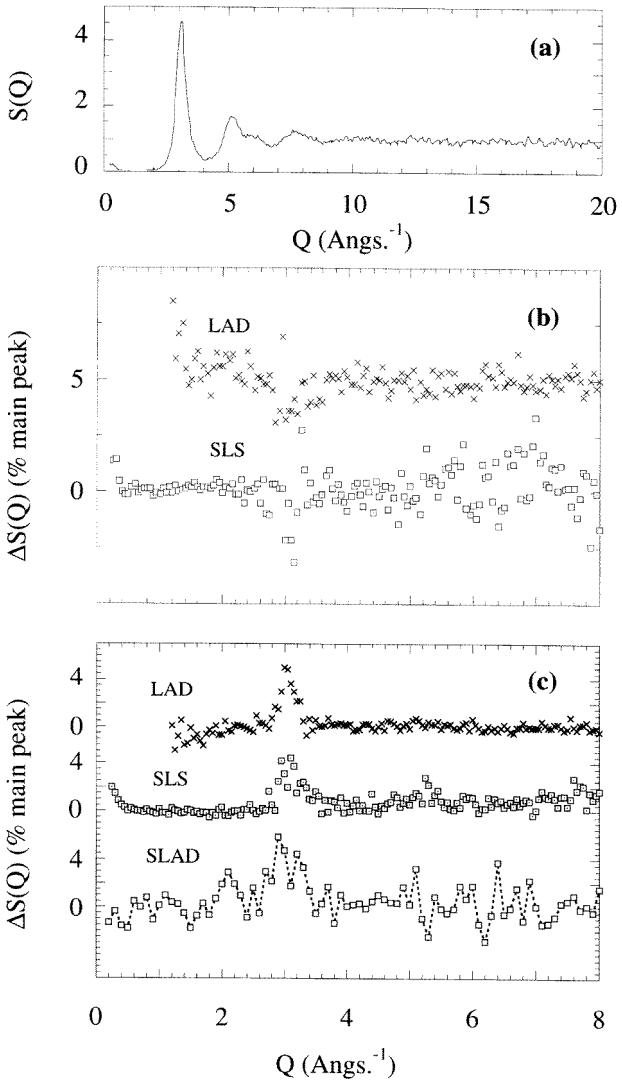

Figure 3. Neutron diffraction data for stress-relieved (SR) and field-annealed (FA) $Fe_{78}Si_9B_{13}$ ribbons from three instruments, LAD and SLS using a spallation source, and SLAD using a reactor source: (a) a representative total structure factor $S(Q)$, (b) $\Delta S(Q) = S(Q_\parallel) - S(Q_\perp)$ for the SR ribbons, and (c) $\Delta S(Q)$ for the FA ribbons.

1 MPa. Similar PDF changes in FeCoSiB metallic glasses have recently been reported [14]. Data analysis using a three-shell Fe–B, Fe–Si and Fe–Fe model for the first-nearest-neighbour pairings gave parameters for the pair distances R_i. The Fe–B pair distances were slightly larger in the FA ribbon than the SR ribbon, 2.14 Å compared with 2.11 Å, while the Fe–Si and Fe–Fe distances were marginally smaller, 2.31 Å compared with 2.33 Å for Fe–Si and 2.48 Å compared with 2.49 Å for Fe–Fe.

Neutron diffraction data are shown in figure 3. To avoid any inconsistencies due to small variations in detector efficiency on LAD and SANDALS, all comparisons between

$S(Q_\parallel)$ and $S(Q_\perp)$ runs were confined to data collected in the same detector. Although the data for the SR ribbon are noisier than the corresponding x-ray patterns because of shorter counting times, a bimodal oscillation is apparent in the neutron data at $\sim$3 Å^{-1} that is similar to that seen in the x-ray data. The $\Delta S(Q)$ patterns for the FA samples show a peak at $Q \approx 3$ Å^{-1}, of magnitude $\sim$5% of the main peak height. In the better-resolved data of the SANDALS experiment, additional features are seen, with peaks at $\sim$5 Å^{-1} and 7.5 Å^{-1}. A sharp upturn is also apparent for Q below $\sim$0.5 Å^{-1}, although it should be noted that SANDALS is not optimized at these very low values of Q, and coherent inelasticity effects might be relevant there. SLAD data are shown for the sample positioned with its normal at $\alpha = 15^\circ$ to the beam so that the scattering vector was in the plane at $|Q| = 2.93$ Å^{-1}. Although the statistical scatter of the SLAD data is greater than for the other instruments, a peak of magnitude $\sim$5% is clearly discernible at $\sim$3 Å^{-1}, with possibly another smaller peak at $\sim$2 Å^{-1}, and a downturn towards negative $\Delta S(Q)$ below $\sim$0.5 Å^{-1}.

Three further SLAD runs (not shown) indicated that the peak in $\Delta S(Q)$ at $\sim$3 Å^{-1} was largest when the scattering vector with $|Q| = 3$ Å^{-1} was in the plane ($\alpha = 15^\circ$), reduced when it was 10° out of the plane ($\alpha = 5^\circ$), and not measurable when it was 15° out of the plane ($\alpha = 0^\circ$ and 30°). Demagnetization effects and the thermal treatment received by the FA ribbons are known to result in a nearly planar distribution of moment directions, as measured by Mössbauer spectroscopy [15]. Given this, the variable-angle SLAD results imply that the peak at $\sim$3 Å^{-1} is magnetic in origin, and due to anisotropy confined in the ribbon plane.

The $\Delta S(Q)$ obtained from all three neutron instruments are self-consistent. The $\Delta S(Q)$ for the SR ribbons appears to be the same as in the x-ray diffraction experiment, so any features may be attributed to structural, and not magnetic, anisotropy. $\Delta S(Q)$ for the FA ribbons is larger than that seen for the x-ray data, and has a different shape, arising from an additional contribution due to magnetic anisotropy. It is the shape of this magnetic $\Delta S(Q)$ contribution, with its small positive peak at $Q \sim 3$ Å^{-1}, that is *the most significant result of this work*, and has important ramifications regarding our microscopic understanding of anisotropy in metallic glasses. In the remainder of this communication we discuss the magnetic $\Delta S(Q)$ peak. We begin by referring to familiar results obtained using polarized neutrons, in order to highlight how and why the current experiments are substantively different from polarized neutron experiments, and may therefore deliver hitherto unmeasured data. We then draw attention to the *sign* of the $\Delta S(Q)$ peak, and show that it signifies the preferential alignment of some moments *perpendicularly* to the anneal field direction. We conclude by considering the interpretation of these results, with reference to the presence of antiferromagnetically coupled moments within the disordered glass structure.

The shape of the $\Delta S(Q)$ pattern for the FA sample resembles the results of polarized neutron scattering experiments on as-cast ribbons of $Fe_{83}B_{17}$ in a saturating field of 1.0 T [16], and amorphous iron (obtained by decomposition of $Fe(CO)_5$ under electric discharge) in an applied field of 1.7 T [17]. In those studies the differences $d\sigma^+/d\Omega - d\sigma^-/d\Omega$ in the scattering cross sections for the two incident polarized neutron states gave large peaks (up to $\sim$65% of the main peak height in amorphous iron [17]) at the same positions as the peaks in the total structure factor. In both cases the peaks were attributed to the magnetic structure factor, which is proportional to the product of the non-magnetic structure factor and the magnetic form factor. The latter varies smoothly from value 1 at $Q = 0$ Å^{-1} to zero at large Q in an exponential-like decay [18, 19], so the magnetic structure factor reflects the peaks in the total structure factor.

Because of the special detector geometries used in our neutron experiments, the $\Delta S(Q)$ that we obtain is similar in origin to the difference signal obtained with polarized neutrons.

However, there are two important differences which explain the small amplitudes of the $\Delta S(Q)$ spectra in figure 3(c) compared to polarized neutron data. First, our experiments are performed in zero field, and therefore we measure the residual magnetic anisotropy due to the field anneal, rather than that induced by an applied magnetic field. This may be a significant difference, since in the zero-field state the individual atomic magnetic moments are likely to exhibit some degree of directional disorder, while in a large applied field the moments will, at least to a first approximation, align parallel to the external field. Second, our experiments use orthogonal in-plane scattering vectors $Q_{\parallel}$ and $Q_{\perp}$ rather than the antiparallel alignment of the polarized neutron states. This allows a more subtle measurement of the in-plane anisotropy.

The sign of the $\Delta S(Q)$ peak is particularly intriguing. It is a feature of the magnetic scattering of unpolarized neutrons from magnetic atoms that the neutrons only 'see' the component of magnetization perpendicular to the scattering vector. From Bitter imaging experiments it is known that the primary domain pattern obtained in FA ribbons comprises walls parallel to the anneal field direction, approximately 100 μm apart [2]. It might therefore seem reasonable to assume that in the FA ribbon the individual atomic moments are aligned collinearly with the anneal field direction. If this is the case we would expect $S(Q_{\parallel})$ to vary as $|F_n|^2$, and $S(Q_{\perp})$ to vary as $|F_n|^2 + |F_m|^2$, where F_n and F_m are the nuclear and magnetic structure factors respectively, so $\Delta S(Q) = S(Q_{\parallel}) - S(Q_{\perp})$ should show *negative* features as evidence for the magnetic contribution. By the same reasoning, we would expect that in the SR ribbons, where the domains lie along the long axis of the ribbon, $\Delta S(Q)$ should show positive magnetic features. At first sight it seems difficult to reconcile these predictions with the experimental observations in figure 3.

However, we must recall that neutron scattering is unique in its ability to genuinely probe the atomic scale structures of the alloy, and that macroscopic techniques such as Bitter domain imaging only reveal the average behaviour of the magnetic atoms. It is certain that there is a reasonable distribution in Fe–Fe distances in the ribbon, as demonstrated for example by our EXAFS data, so we may expect some degree of local fluctuation in the magnetic structure. Also, the neutron scattering signature for magnetic correlations on the micron to millimetre scale, corresponding to the domain structure, is well known to occur at low Q-values, below $\sim$1 Å^{-1}. With this in mind, and accepting that the SANDALS diffractometer is not optimized for measurements in that Q-range, whereas the SLAD diffractometer is, the data in figure 3(c) for the FA ribbons are consistent with the presence of a negative $\Delta S(Q)$ at low Q due to the domain structure. This leaves open the question of the origin of the relatively large positive $\Delta S(Q)$ peak at $\sim$3 Å^{-1} in the FA ribbons. There is no doubt that it is real: three independent measurements on three different neutron diffractometers attest to that. What is clear is that (i) it is a *magnetic* feature, (ii) it arises from moments that to some extent lie *perpendicularly* to the anneal field direction, and (iii) it occurs at the position of the main $S(Q)$ peak and is therefore associated with *local* structure.

We propose the following interpretation of these results, as a self-consistent account of this programme, and also to set them in the context of other research. In many magnetic studies of $Fe_{78}Si_9B_{13}$ evidence has been found for 'moment canting', a phenomenon where the Fe moments do not completely align either spontaneously or in the presence of high fields [6, 15, 20]. To explain this, an *a priori* model was suggested for the moment canting due to frustrated exchange interactions between some of the magnetic atoms [6]. It was shown that antiferromagnetically coupled Fe–Fe pairs can give rise to substantial long-range perturbations in the so-called 'combed hair' effect [6]. We take this model as the essential feature of the spin structure in such amorphous ferromagnets.

Heat treatment (with or without an applied field) is known from dilatometric studies [21] to lead to densification, which must reduce the average nearest-neighbour distances. For Fe, a reduction in nearest-neighbour spacing will drive the exchange towards antiferromagnetism; the position of Fe on the Bethe–Slater curve is the simplest support for this argument. In the absence of an applied field during annealing, the direction of any antiferromagnetic spin pair is arbitrary, and thus the net direction of the 'combed hair' perturbation is arbitrary for each frustrated site. This will therefore tend to produce a material with no net *macroscopic* easy direction. With an applied field present, the atomic rearrangements which lead to densification, and the generation of further frustrated spins, is biased by the direction of the applied field, and a net *macroscopic* anisotropy is introduced. The structural anisotropy may therefore come from the field-biased shearing of the structure and local magnetoelastic distortions of the structure. Moreover, the positive sign of the $\Delta S(Q)$ peak is consistent with antiferromagnetically coupled pairs or clusters of moments preferentially aligning with their coupling directions perpendicular to the anneal field direction. This is analogous to a spin-flop response, with the moments reorienting and canting in response to the applied field.

An important earlier finding [2] was that the direction of the *macroscopic* easy axis is quickly established, but the magnitude of the anisotropy develops over a more protracted period. This is not inconsistent with our interpretation. As soon as antiferromagnetic pairs are created by local atomic rearrangements, a direction, that of the applied field, is established. Under longer thermal treatment the 'combed hair' pattern is stabilized by longer-range diffusive rearrangements of atoms, increasing the associated anisotropy energy density.

We thank the instrument scientists at Daresbury, Graham Bushnell-Wye and Bob Bilsborrow, and at ISIS, Spencer Howells and Alan Soper, and acknowledge the assistance of the UK Engineering and Physical Sciences Research Council, through grants GR/H28073 and GR/J97618. LFB thanks the Spanish Ministry of Science (MEC) for an FPU postdoctoral grant. JDW thanks the Lloyds of London Tercentenary Foundation for the award of a postdoctoral fellowship.

References

[1] Barandiarán J M, Hernando A, Madurga V, Nielsen O V, Vázquez M and Vázquez Lopez M 1987 Temperature, stress, and structural relaxation dependence of the magnetostriction in $(Co_{0.94}Fe_{0.06})_{75}Si_{15}B_{10}$ glasses *Phys. Rev.* B **35** 5066–71

[2] Thomas A P and Gibbs M R J 1992 Anisotropy and magnetostriction in metallic glasses *J. Magn. Magn. Mater.* **103** 97–110

[3] Dini K, Cowlam N and Davies H A 1982 A comparison of structural measurements on Fe–B metallic glasses *J. Phys. F: Met. Phys.* **12** 1553–66

[4] Dini K, Cowlam N, Gregan G P and Davies H A 1986 A comparison of structural relaxation in $Ni_{64}B_{36}$ and $Fe_{83}B_{17}$ metallic glasses *Can. J. Phys.* **64** 658–64

[5] Spilsbury D, Cowlam N, Howells W S and Davies H A 1995 The continued search for structural anisotropy in metallic glass ribbon *Key Eng. Mater.* **103** 231–4

[6] Pankhurst Q A, Jiang J Z, Betteridge S, Gibbs M R J and Gehring G A 1995 Moment canting in amorphous FeSiB ribbons in applied fields: unpolarized Mössbauer effect studies *J. Phys.: Condens. Matter* **7** 9571–93

[7] Thomas A P, Gibbs M R J and Squire P T 1990 Dependence of magnetostriction on induced anisotropy in metallic glasses *IEEE Trans. Magn.* **26** 1406–8

[8] Fdez-Gubieda M L, Orue I, Plazaola F and Barandiarán J M 1996 Evidence of strong short-range order in $(Fe_{0.2}Co_{0.8})_{75}Si_xB_{25-x}$ amorphous alloys from EXAFS spectroscopy *Phys. Rev.* B **53** 620–8

[9] Bushnell-Wye G and Cernik R J 1992 The general purpose 2-circle diffractometer on Station 9.1, Daresbury Laboratory *Rev. Sci. Instrum.* **63** 999–1001

[10] Pankhurst Q A, Wicks J D and Gibbs M R J 1995 Structural and magnetic anisotropy in field-annealed FeSiB amorphous alloy *ISIS Annual Report 1995* vol 2, ed C Wilson (Swindon: Swindon Press) p A348
[11] Windsor C G, Boudreaux D S and Narasimhan M C 1978 A search for anisotropy in the structure factor of amorphous $Pd_{0.8}Si_{0.2}$ ribbon *Phys. Lett.* **67A** 282–4
[12] Suzuki Y, Haimovich J and Egami T 1987 Bond-orientational anisotropy in metallic glasses observed by x-ray diffraction *Phys. Rev.* B **35** 2162–8
[13] Tomida T and Egami T 1993 Molecular-dynamics study of structural anisotropy and anelasticity in metallic glasses *Phys. Rev.* B **48** 3048–57
[14] Fdez-Gubieda M L, Orue I and Plazaola F 1995 EXAFS and Mössbauer studies of short range order changes related to magnetic anisotropy induction in metallic glasses *Nanostructured and Non-Crystalline Materials*, ed M Vazquez and A Hernando (Singapore: World Scientific) p 389
[15] Jiang J Z, Pankhurst Q A and Gibbs M R J 1995 The effect of field annealing on moment canting in amorphous $Fe_{78}Si_9B_{13}$ *J. Magn. Magn. Mater.* **144** 323–4
[16] Cowlam N and Carr G E 1985 Magnetic and structural properties of Fe–B binary metallic glasses. 2. Magnetic neutron scattering experiments *J. Phys. F: Met. Phys.* **15** 1117–26
[17] Schweizer J 1982 Polarized neutron scattering studies on amorphous solids *Nucl. Instrum. Methods* **199** 115–23
[18] Lisher E J and Forsyth J B 1971 Analytical approximations to form factors *Acta Crystallogr.* A **27** 545–50
[19] Blétry J and Sadoc J F 1975 Determination of the three partial interference functions of an amorphous cobalt–phosphor ferromagnet by polarized neutron scattering *J. Phys. F: Met. Phys.* **5** L110–7
[20] Graham C D Jr and Gibbs M R J 1993 High-field magnetization of metallic glasses *IEEE Trans. Magn.* **29** 3457–9
[21] Gibbs M R J and Sinning H R 1985 A critique of the roles of TSRO and CSRO in metallic glasses by application of the activation-energy spectrum model to dilatometric data *J. Mater. Sci.* **20** 2517–25